

## Evaluation of Lane Keeping Assistance Controllers in HIL Simulations

Junyeon Hwang\*, Kunsoo Huh\*\*  
Hyukmin Na\*\*\*, Hogi Jung\*\*\*, Hyungjin Kang\*\*\*, Paljoo Yoon\*\*\*

\*Dept. Of Automotive Engineering, Hanyang University, Seoul, Korea  
(e-mail: gbhwang@hanyang.ac.kr).

\*\* Dept. Of Automotive Engineering, Hanyang University, Seoul, Korea  
(Tel: 082-2-2220-0437; e-mail: khuh2@hanyang.ac.kr)

\*\*\* Central R&D Center, Mando Corporation, Korea  
(e-mail: [hyuckmin@mando.com](mailto:hyuckmin@mando.com), [hjung@mando.com](mailto:hjung@mando.com), [hjkang@mando.com](mailto:hjkang@mando.com), [pjyoon@mando.com](mailto:pjyoon@mando.com))

**Abstract:** Lane Keeping Assistant Systems (LKAS) require the cooperative operation between drivers and active steering angle/torque controllers. An LKAS system is proposed in this study such that the desired path is generated to minimize the trajectory overshoot. Based on the reference path, an optimal controller is designed to minimize the cost function. A HIL (Hardware In the Loop) simulator is constructed to evaluate the proposed LKAS system. The single camera is mounted on the simulator and acquires the monitor images to detect lane markers. The performance of the proposed system is evaluated by HIL system using the Carsim and the Matlab Simulink.

### 1. INTRODUCTION

The intelligent vehicle systems are intended to improve the driving safety and convenience by utilizing the state-of-art mechanical, electric/electronic, control and communication technology. Lane Keeping Assistance System (LKAS) is one of the intelligent vehicle's functions, which assists lane keeping for drivers and provides convenient driving circumstance with LDW (Lane Departure Warning).

Many researches have been carried out in the LKAS field (Horiuchi and Sunada, 1998, KoSeck et al, 1998, Nagai et al, 2002, Rossetter et al, 2004, Shimakage et al, 2002, et al). These systems can keep the lane by controlling the angle of vehicle's steering wheel or by generating the torque on steering wheel. The subjective viewpoint of driver was investigated (Omae and Shimizu, 2006) with various LKAS controllers, which shows that the performance superiority does not necessarily match the driver's receptiveness. In operating the LKAS system, an excessive control input can cause the overshoot in vehicle's lateral position.

In this paper, an LKAS system is proposed by adopting the desired reference path generation algorithm and the optimal control technique. The cost function includes the heading angle error, lateral offset and assisted torque size. The steering torque outputs from the LKAS and the EPS are added together and their sum is delivered to the driver. The size of the sum should be small enough for the driver to easily override the steering command.

In order to evaluate the performance of the proposed system, a HIL (Hardware In the Loop) simulator is built using the Carsim software and the Matlab Simulink. The single camera is used to acquire the monitor image and to calculate the lane information. The heading angle error and the lateral offset are

obtained from the lane markers in front, which are detected using the vision sensor.

### 2. THE SYSTEM STRUCTURE

Figure 1 shows the system's overall structure. The vision system can calculate the vehicle position parameters such as the heading angel and lateral offset. The vehicle motion parameters such as yaw velocity and lateral velocity are assumed to be measured or calculated from the vehicle motion sensors. The dotted box at the top of Fig.1 represents steering wheel model and vehicle model, respectively. The dotted box at the bottom of Fig.1 is the designed controller which includes the LKAS system and EPS logic. In this paper, the LKAS controller is designed using the optimal control technique and the EPS uses commercial EPS logics.

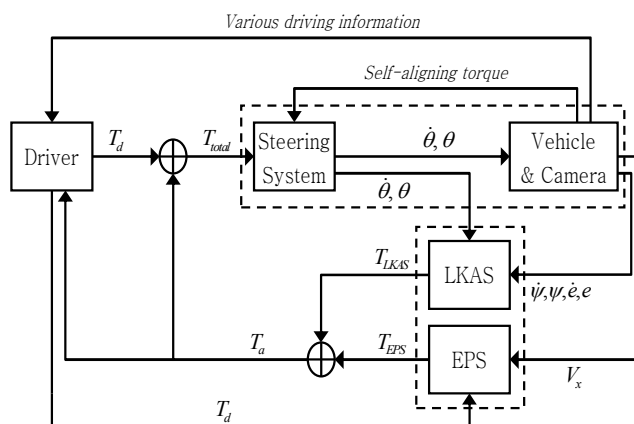


Fig. 1. The overall structure

The LKAS calculates the driver assist torque by using the information from the vision system and vehicle sensors, and the EPS generates the assist torque based on the driver torque and vehicle longitudinal speed. The driver can feel the assist torque from the touch of the steering wheel. By looking at the vehicle's movement, the driver, in turn, can generate a appropriate torque using the information of vehicle's movement.

### 2.1 Vehicle Model

In this paper, a bicycle vehicle model, shown in Fig.2, is used and can be expressed as follows (Rajamani, 2006).

$$\begin{aligned} m(\ddot{y} + V_x \dot{\psi}_c) &= 2F_f + 2F_r \\ I_z \ddot{\psi}_c &= 2l_f F_f - 2l_r F_r \end{aligned} \quad (1)$$

where  $y$  is the lateral displacement;  $V_x$  is the vehicle speed,  $\psi_c$  is the yaw angle;  $I_z$  is the yaw moment of inertia;  $m$  is the vehicle mass;  $F_f$  ( $F_r$ ) is the cornering force at the front (rear) tire;  $l_f$  ( $l_r$ ) is the distance from c.g. to the front (rear) axle.

Assuming that the lateral acceleration is small, we can use the simplified tire model as shown in (2)

$$\begin{aligned} F_f &= C_f \left( \delta - \frac{\dot{y} + l_f \dot{\psi}_c}{V_x} \right) \\ F_r &= C_r \left( -\frac{\dot{y} - l_r \dot{\psi}_c}{V_x} \right) \end{aligned} \quad (2)$$

where  $\delta$  is the front steering angle.  $C_f$  and  $C_r$  are cornering stiffness of front and rear tires, respectively. The above equations can be modified to represent the relative position and angle of the vehicle with respect to road. In Fig. 2,  $e$  is the lateral offset between the lane and the vehicle center,  $\psi$  is the heading angle between the lane and the vehicle's leading direction. When the vehicle is turning on the road with the road curvature of  $1/R$  and the velocity of  $V_x$ , the vehicle's desired yaw rate can be expressed as follows.

$$\dot{\psi}_{des} = \frac{V_x}{R} \quad (3)$$

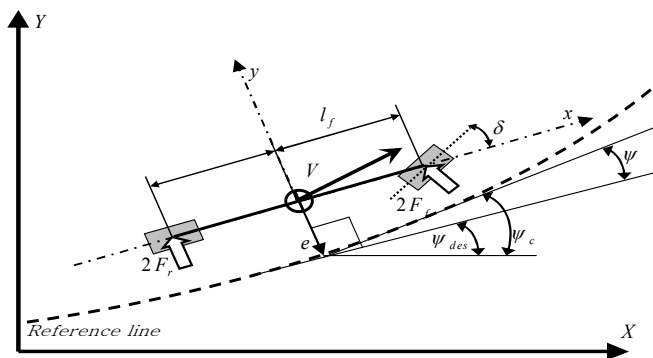


Fig. 2. Lateral vehicle dynamics

The equations of (1), (2) and (3) can be transformed into the state space form as follows,

$$\frac{d}{dt} \begin{bmatrix} \dot{\psi} \\ \psi \\ e \end{bmatrix} = \begin{bmatrix} a_{11} & a_{12} & a_{13} & 0 \\ 1 & 0 & 0 & 0 \\ a_{31} & a_{32} & a_{33} & 0 \\ 0 & 0 & 1 & 0 \end{bmatrix} \begin{bmatrix} \dot{\psi} \\ \psi \\ \dot{e} \\ e \end{bmatrix} + \begin{bmatrix} a_{16} \\ 0 \\ a_{36} \\ 0 \end{bmatrix} \delta + \begin{bmatrix} b_{12} \\ 0 \\ b_{32} \\ 0 \end{bmatrix} \dot{\psi}_{des} \quad (4)$$

$$a_{11} = \frac{-2(C_f l_f^2 + C_r l_r^2)}{I_z V_x}, \quad a_{12} = \frac{2(C_f l_f - C_r l_r)}{I_z}$$

$$a_{13} = \frac{-2(C_f l_f - C_r l_r)}{I_z V_x}, \quad a_{31} = \frac{2(-C_f l_f + C_r l_r)}{m V_x}$$

$$a_{32} = \frac{2(C_f + C_r)}{m}, \quad a_{33} = \frac{-2(C_f + C_r)}{m V_x}$$

$$a_{16} = \frac{2C_f l_f}{I_z}, \quad b_{12} = \frac{-2(C_f l_f^2 + C_r l_r^2)}{I_z V_x}$$

$$a_{36} = \frac{2C_f}{m}, \quad b_{32} = \frac{2(-C_f l_f + C_r l_r)}{m V_x} - V_x$$

### 2.2 Steering System Model

Figure 3 illustrates the steering wheel mechanism used in this study and its motion can be expressed as follows.

$$\left( I_{sw} + \frac{I_s}{N^2} \right) \ddot{\theta} = -(C_{sw} + C_s) \dot{\theta} - \frac{T_s}{N} + T_a + T_d \quad (5)$$

where  $\theta$  is the steering angle;  $T_s$  is the self-aligning torque;  $T_a$  is the assist torque;  $T_d$  is the driver torque;  $I_{sw}$  is the moment of inertia of steering wheel;  $C_{sw}$  is viscous friction coefficient of steering wheel;  $I_s$  is the equivalent moment of

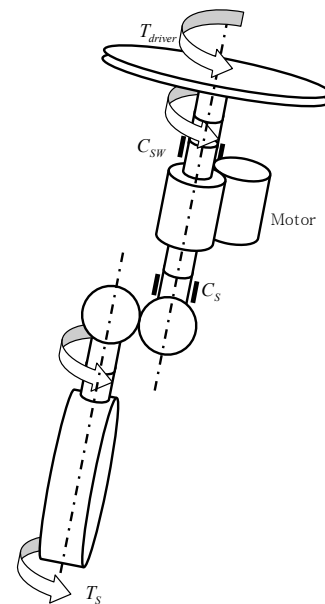


Fig. 3. Steering wheel mechanism

inertia of front wheel;  $C_s$  is the equivalent viscous friction coefficient of front wheel; and  $N$  is the steering gear ratio.

The self-aligning torque can be obtained from,

$$T_s = 2\xi F_f \quad (6)$$

where  $\xi$  is the front wheel trail.

### 2.3 Combined System

From the bicycle vehicle model and the steering mechanism model, the state equation can be obtained for designing a state feedback controller. The steering torque is included as a control input.

$$\frac{d}{dt} \begin{bmatrix} \dot{\psi} \\ \psi \\ \dot{e} \\ e \\ \dot{\theta} \\ \theta \end{bmatrix} = \begin{bmatrix} a_{11} & a_{12} & a_{13} & 0 & 0 & a'_{16} \\ 1 & 0 & 0 & 0 & 0 & 0 \\ a_{31} & a_{32} & a_{33} & 0 & 0 & a'_{36} \\ 0 & 0 & 1 & 0 & 0 & 0 \\ a_{51} & a_{52} & a_{53} & 0 & a_{55} & a_{56} \\ 0 & 0 & 0 & 0 & 1 & 0 \end{bmatrix} \begin{bmatrix} \dot{\psi} \\ \psi \\ \dot{e} \\ e \\ \dot{\theta} \\ \theta \end{bmatrix} + \begin{bmatrix} 0 \\ 0 \\ 0 \\ 0 \\ b_{51} \\ 0 \end{bmatrix} (T_a + T_d) \quad (7)$$

$$\begin{aligned} a'_{16} &= \frac{a_{16}}{N}, & a'_{36} &= \frac{a_{36}}{N} \\ a_{51} &= \frac{2\xi C_f I_f}{\left(I_{sw} + \frac{I_s}{N^2}\right) N V_x}, & a_{52} &= -\frac{2\xi C_f}{\left(I_{sw} + \frac{I_s}{N^2}\right) N} \\ a_{53} &= \frac{2\xi C_f}{\left(I_{sw} + \frac{I_s}{N^2}\right) N V_x}, & a_{55} &= -\frac{(C_{sw} + C_s)}{\left(I_{sw} + \frac{I_s}{N^2}\right)} \\ a_{56} &= -\frac{2\xi C_f}{\left(I_{sw} + \frac{I_s}{N^2}\right) N^2}, & b_{51} &= \frac{1}{\left(I_{sw} + \frac{I_s}{N^2}\right)} \end{aligned}$$

Because the radius of curved highway is very large compared to the look-ahead distance of LKAS systems, the desired yaw rate term in (4) can be ignored.

### 2.4 Desired Reference Path Generation (DRPG) method

In general, the center-line of the lane is chosen as the desired reference path in LKAS systems. However, the tracking performance of the controlled vehicle is affected by the accuracy of the vehicle model and the controller robustness. If the controller is designed too aggressive, the excessive control input can cause the overshoot of the trajectory which, in turn, results in the override action from the driver to correct the vehicle motion. On the contrary, if the controller is designed too conservative, it may take long to approach the reference path. Neither case is acceptable from the control perspectives.

In order to improve the above cases, a desired reference path generation algorithm is proposed in this study. As shown in Fig. 4, smooth approach to the centreline can be achieved by tangential curves and its path on each camera image sequence needs to be calculated based on the lane information. The

vehicle speed is assumed constant in this calculation. For the reference path,  $\mathbf{p}_{des}^n$ , of  $n^{th}$  image frame,  $l$  reference points,  $P_1^n, P_2^n, \dots, P_l^n$  are determined to form a tangential curve.

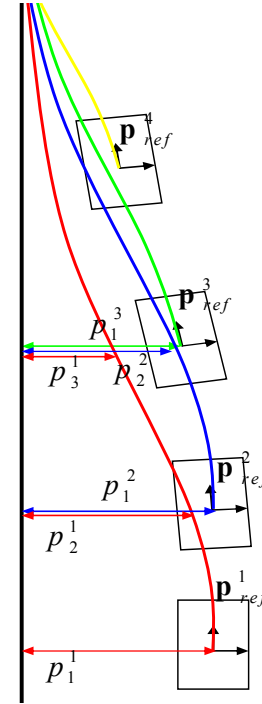


Fig. 4. Desired reference path

This algorithm stores the reference points and path for each image frame and obtains the desired reference path by weighting the previous reference paths.

$$\begin{aligned} \mathbf{p}_{des}^1 &= \mathbf{p}_{ref}^1 = [p_1^1 \ p_2^1 \ \dots \ p_l^1] \\ \mathbf{p}_{des}^2 &= (\mathbf{p}_{ref}^2 \cdot [1 \ 0 \ \dots \ 0]^T + w \mathbf{p}_{ref}^1 \cdot [0 \ 1 \ \dots \ 0]^T) / 2 \\ \mathbf{p}_{des}^3 &= (\mathbf{p}_{ref}^3 \cdot [1 \ 0 \ \dots \ 0]^T + w \mathbf{p}_{ref}^2 \cdot [0 \ 1 \ \dots \ 0]^T + w^2 \mathbf{p}_{ref}^1 \cdot [0 \ 0 \ 1 \ \dots \ 0]^T) / 3 \\ &\vdots \\ \mathbf{p}_{des}^n &= \left( \sum_{i=n-l+1}^n w^{n-i} \mathbf{p}_{ref}^i \cdot \mathbf{I} \right) / l \end{aligned} \quad (8)$$

with

- $w$  : forgetting factor ( $0 \leq w \leq 1$ )
- $p_l^n$  :  $l^{th}$  reference point in the  $n^{th}$  image frame
- $\mathbf{p}_{ref}^n$  : reference path of  $n^{th}$  image frame
- $\mathbf{I}$  :  $l \times l$  identity matrix

### 2.5 LKAS Controller Design

In the LKAS controller design, the optimal control technique is applied to determine the assisted torque to the driver. The cost function is formulated including the heading angle, lateral offset and the assist torque size. The weight functions are decided for the best performance.

$$J = \int_0^{\infty} (q_2 \psi^2 + q_4 e^2 + T_a^2) dt \quad (9)$$

$$q_2 = q_4 = 10$$

The LQR (Linear Quadratic Regulator) controller is designed to minimize the above function and is expressed as the state feedback as follows.

$$u = T_a = -Kx \quad (10)$$

$$= -(k_1 \dot{\psi} + k_2 \psi + k_3 \dot{e} + k_4 e + k_5 \dot{\theta} + k_6 \theta)$$

where  $K$  is the state feedback controller gain.

### 3. SIMULATIONS

In order to evaluate the performance of the proposed LKAS system, a HILS simulator is constructed as shown in Fig. 5. The software of the HILS was designed based on the Matlab Simulink and the Carsim. The steering wheel unit is composed of torque sensor, potentiometer and two motors. The torque sensor measures driver torque and the potentiometer measures the steering wheel angle. The two motors in Fig. 6 work with the Carsim software and driver's steering command. The motors generate the vehicle's self-aligning torque, the calculated LKAS torque and the EPS torque from the commercial EPS logic.

The vision system is mounted on the simulator as shown in the Fig. 5 and the camera is mounted parallel to the horizontal direction of the monitor image. The Carsim software supports the camera view where the camera calibration information is included such as camera position, rotation and field of view. The camera can acquire the monitor images in real time to detect the lane markers. The lane detection method (Huh et al, 2005) is utilized with the image of  $640 \times 480$  pixel size. The calculation time for one frame is about 0.003sec and the image grabbing rate is 30fps. The lane detection system was developed with Labview language and IEEE 1394 CMOS camera. Two road models are considered depending on the look-ahead distance in order to obtain the vehicle position, heading angle, road curvature.

#### 3.1 Simulation Environment

The simulation is carried out for driver only mode and for the LKAS control mode, respectively. The driving course includes left and right curved route with 5000m length as shown in Fig. 7. The road scene is created using real road data as shown in Fig. 8 with the lane width of 3.7m and the road curvature of about 500m. The vehicle speed in the simulation is set to 80Km/h for comparison. The lane keeping performance and the workload of the driver are compared using the following performance index (Nagai et al, 2002).

$$LP = \int_0^t e^2 dt \quad (11)$$

$$PW = \int_0^t T_d^2 dt \quad (12)$$

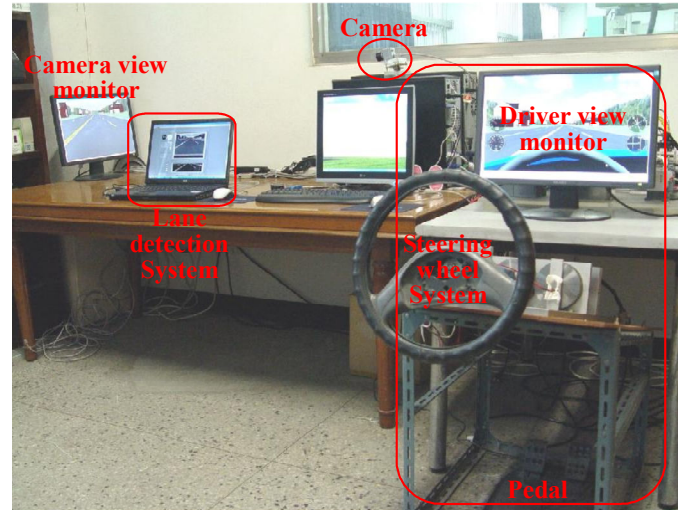


Fig. 5. HILS Simulator

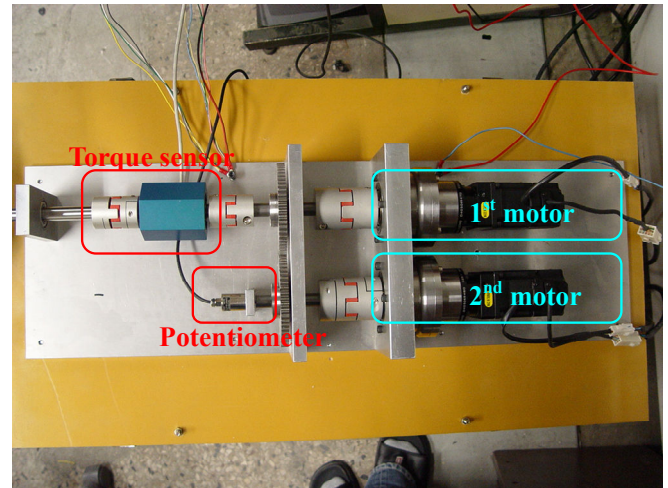


Fig. 6. Steering wheel unit

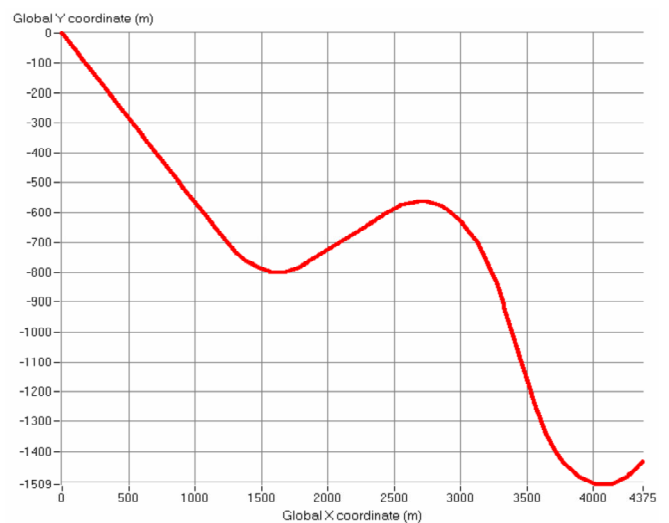


Fig. 7. Road course in driving simulator



Fig. 8. Simulation road scene

### 3.2 Verification of Lane Detection method

In order to verify the lane detection method, the lateral offset results are evaluated first. The calculated lateral offset based on the lane detection method is compared with the Carsim data as shown in Fig. 9. The calculated lateral offset is very close to true values except a time delay.

### 3.3 LKAS Results

The lane tracking performance with the LKAS system is evaluated in the HILS simulator. As listed in Table. 1, the LKAS system provides better lane tracking performance with less workload on the driver.

Figure 10 shows that the LKAS assisted driver applies less torque than the driver only does, which demonstrates the driver workload improvement. The lane keeping improvement is illustrated in Fig. 11 where lateral offset is decreased significantly with the LKAS assisted driver. The LKAS with the proposed DRPG algorithm shows a little better performance than the LKAS without the DRPG algorithm. The both controllers have similar results in driver workload improvement but the LKAS with the DRPG algorithm shows less lateral offset. As illustrated in Fig. 11, the LKAS with the DRPG algorithm induces less overshoot when the vehicle crosses the lane center.

Table. 1. Simulation results

Index	LP( $m^2s$ )	PW( $N^2m^2s$ )
Driver only	30.98	313.24
LKAS without DRPG method	13.03	232.87
LKAS with DRPG method	8.68	223.74

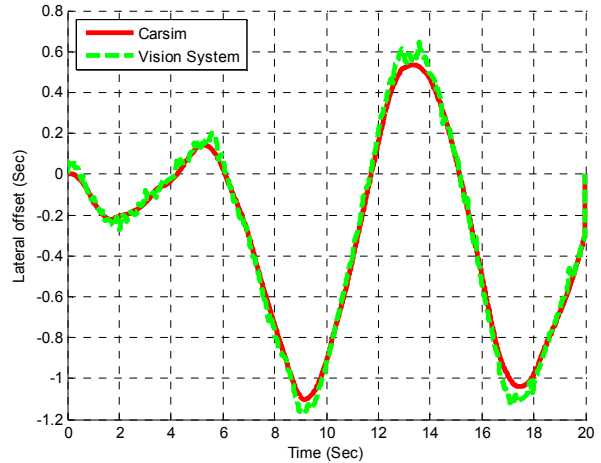


Fig. 9. Lateral offset from the vision system

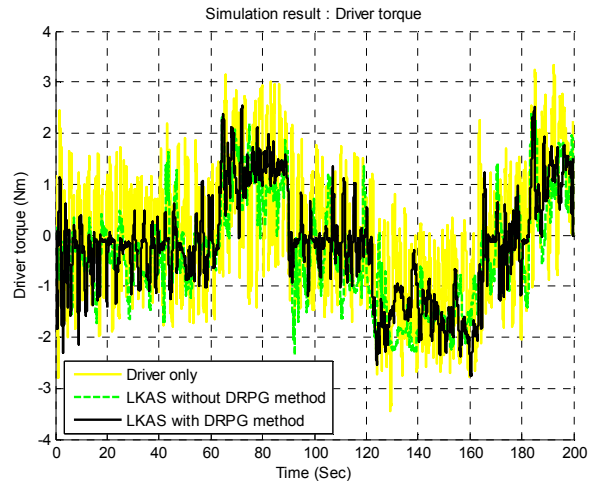


Fig. 10. Simulation results (driver torque)

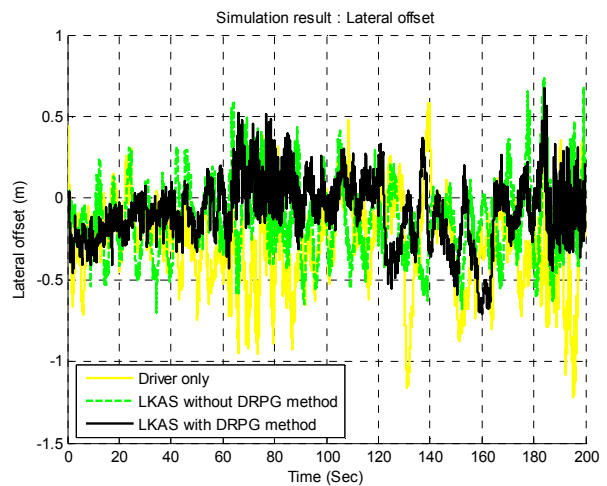


Fig. 11. Simulation results (lateral offset)

#### 4. CONCLUSIONS

In this paper, an LKAS (Lane Keeping Assistance System) controller is designed in order to provide convenient lane keeping and to reduce driver workload. The vision system is included to detect lane markers and to calculate the lateral offset. The reference path generation algorithm is proposed to minimize the overshoot of the controlled vehicle. The HILS simulations are carried out with three modes of driver only, LKAS with and without the DRPG algorithm, respectively.

The simulation results demonstrate that the LKAS controller reduces lateral offset of a vehicle and driver's workload. The LKAS with the DRPG algorithm works more effectively than LKAS without the DRPG algorithm by decreasing the lateral offset overshoot when the vehicle crosses the lane center.

#### REFERENCES

- Horiuchi. S. and Sunada. K. (1998). Synthesis of Driver Assistance System for Lane-Following Using Generalized Predictive Control, Proc. of AVEC'98, pp 467-472
- KoSeck. J., Blasi. R., Taylor. C. J. and Malik. J. (1998). A Comparative Study of Vision-Based Lateral Control Strategies for Autonomous Highway Driving, Proceedings of the 1998 IEEE, International Conference on Robotics & Automation, pp 1903-1908
- Leelavansuk, P., Shitamitsu. K., Mouri. H., Nagai. M. (2002) Study on cooperative control of driver and Lane-Keeping Assistance system, In Proceedings of the International Symposium on Advanced Vehicle Control (AVEC), pp. 219-224.
- Rosseter. E. J., Switkes. J. P., Gerdes. J. C. (2004) Experimental Validation of the Potential Field Lane keeping System. International Journal of Automotive Technology, vol. 5, No. 2, pp 95-108
- Shimakage. M., Satoh. S., Uenuma. K., Mouri. H. (2002) Design of lane-keeping control with steering torque input, JSAE Rev. 23, pp 317-323
- Omae, M., Shimizu, H. (2006) Comparison of Lane-keep Assists by using Steering Torque, Steering Angular Velocity and Steering Angle, Proceedings of AVEC '06, AVEC060024
- Rajamani. R. (2006) Vehicle Dynamics and Control, Springer
- Huh. K., Park. J., Hong. D., Cho. D.D., Park. J. (2005) Development of a vision-based lane detection system considering configuration aspects. Optics and Lasers in Engineering, vol. 41, no. 11, pp 1193-213
- Bertozzi. M., Broggi. A. (1998) GOLD: A Parallel Real-Time Stereo Vision System for Generic Obstacle and Lane Detection. IEEE Transactions on Image Processing , 7 ,pp 62-81.